INNOSLAB-based single-frequency MOPA for airborne lidar detection of CO_2 and methane

Jens Löhring*[a], Jörg Luttmann[a], Raphael Kasemann[a], Michael Schlösser[a], Jürgen Klein[a], Hans-Dieter Hoffmann[a], Axel Amediek[b], Christian Büdenbender[b], Andreas Fix[b], Martin Wirth[b], Mathieu Quatrevalet[b], Gerhard Ehret[b]

[a]Fraunhofer Institut für Lasertechnik, Steinbachstr. 15, 52074 Aachen, Germany;
[b]Deutsches Zentrum für Luft- und Raumfahrt, Institut für Physik der Atmosphäre, Münchener Str. 20, 82234 Weßling, Germany

ABSTRACT

For the CO_2 and CH_4 IPDA lidar CHARM-F two single frequency Nd:YAG based MOPA systems were developed. Both lasers are used for OPO/OPA-pumping in order to generate laser radiation at 1645 nm for CH_4 detection and 1572 nm for CO_2 detection. By the use of a Q-switched, injection seeded and actively length-stabilized oscillator and a one-stage INNOSLAB amplifier about 85 mJ pulse energy could be generated for the CH_4 system. For the CO_2 system the energy was boosted in second INNOSLAB-stage to about 150 mJ. Both lasers emit laser pulses of about 30 ns pulse duration at a repetition rate of 100 Hz.

Keywords: LIDAR, IPDA, single frequency, Nd:YAG, MOPA, INNOSLAB

1. INTRODUCTION

The INNOSLAB architecture has demonstrated its advantages and potential as a power amplifier as part of MOPA arrangements in different parameter fields within the past few years. On the one hand mode coupled laser sources with pulse durations in the picosecond and femtosecond regime were boosted up to the kW-level mean power [1]. On the other hand this scheme has successfully been applied to the amplification of nanosecond laser pulses to the 100 mJ level at high efficiencies [2][3]. Typically, the latter parameter field has to be addressed in the field of atmospheric remote sensing where the LIDAR technology is applied. One special application in this field is the determination of column averaged volume mixing ratios of CH_4 (XCH_4) and CO_2 (XCO_2) especially for climate research. For this goal the airborne CHARM-F (CO_2 and CH_4 Atmospheric Remote Monitoring – Flugzeug) IPDA (Integral Path Differential Absorption) was developed for DLR's new High-Altitude, LOng-range research aircraft, HALO. The CHARM-F instrument was designed for purely scientific, non-commercial purposes. This article will focus on the Nd:YAG based MOPA that is used for pumping the nonlinear frequency converters. The light pulses at the gas-specific absorption wavelength of 1645 nm and 1572 nm are generated in optical parametrical oscillators (OPO) and amplifiers (OPA) pumped at 1064 nm. More details about the CHARM-F-system and its appropriate frequency converters (OPO/OPA) were published elsewhere [4]..[10].

Currently, a preliminary design for a spaceborn CH_4-IPDA-instrument is under investigation within the French-German MERLIN (**Me**thane **R**emote Sensing **LI**DAR Missio**n**) project [11][12]. The baseline architecture for the MERLIN-laser transmitter is inherited from the CH_4-path of the CHARM-F-system and consists of a downsized stable low energy oscillator, one INNOSLAB-amplifier stage and a subsequent OPO-converter. Therefore, the CHARM-F system plays an important role as a technology demonstrator for MERLIN.

*jens.loehring@ilt.fraunhofer.de; phone +49 241 8906-673; fax +49 241 8906-121; ilt.fraunhofer.de

2. SETUP

2.1 Optical setup

The pump radiation of the CHARM-F laser sources is generated in different steps (see Figure 2-1). The spectral, temporal and the main spatial beam properties are generated in a low energy quality switched and injection seeded Nd:YAG based oscillator. Firstly, the pulse energy is boosted in one subsequent INNOSLAB amplifier stage to the 75 mJ level. In the CO_2 system the pulse energy is doubled in a second amplifier stage to the 150 mJ level. In the CH_4-system the pump beam is converted into the measurement radiation at 1645 nm wavelength in one optical parametrical oscillator (OPO) stage. In the CO_2 system a multistep frequency conversion process which comprises an OPO and an OPA (optical parametrical amplifier) stage or alternatively a high power OPO stage will be applied. This manuscript focusses on the properties of the pump laser chain. The frequency conversion scheme will be presented elsewhere [10]. For the measurements about 10 mJ and 30 mJ are required, respectively.

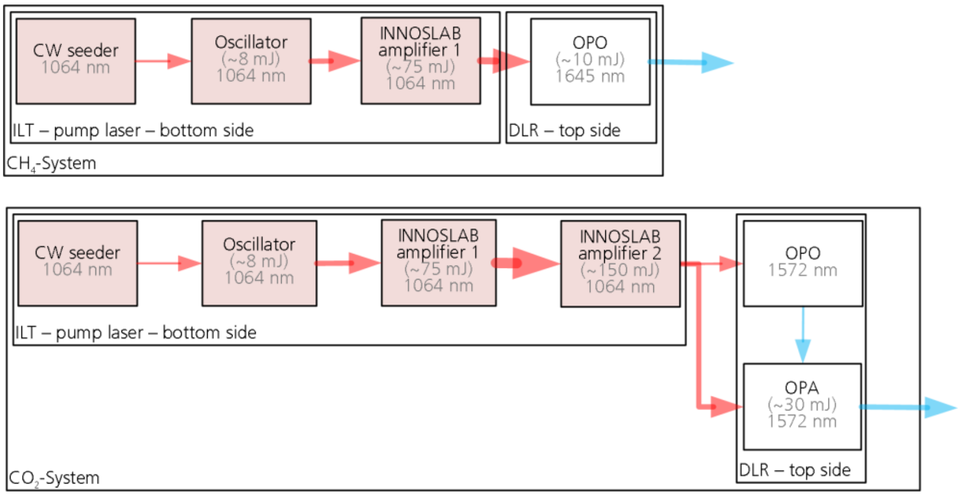

Figure 2-1: General scheme for beam generation of the CHARM-F system. The pump beam is generated in different stages and is subsequently converterd to the measurement radiation. Within this document only the pump laser systems (red boxes) are described in detail.

An illustration of the oscillator section is given in Figure 2-2. The most relevant oscillator properties are listed in Table 2-1. The laseractive medium is a slab shaped Nd:YAG crystal which is longitudinally pumped from both end faces. For pumping, fiber coupled diode laser modules at 808 nm wavelength are used. The appropriate output facets of the fibers are imaged with two-lens telescopes into the crystal. Pump light and laser light are separated by a dichroic mirror on both optical crystal apertures. For cooling the laser crystal is soldered into a copper heat sink. For compactness reasons, the optical path is folded one time between the outcoupler and the laser crystal. Active high quality switching is done with a setup comprising a thin film polarizer, pockels cell and quarterwave plate. The polarizer is used as mirror. The end mirror is mounted on a piezo actor for cavity length control.

A spectrally narrowband cw-laser signal of about 10 mW from a commercially available fiber laser source is transversally modematched and coupled through the polarizer into the cavity. To ensure spectrally stable emission the fiber laser is protected from noise signal coming from the oscillator by a Faraday isolator which offers a damping of more than 30 dB. In order to generate single frequency pulses the oscillator cavity length has to be in resonance with the cw-seed signal. For this, the Ramp&Fire-technique is applied where the transmission of the seed signal through the cavity is measured with a photodiode behind the second folding mirror behind the outcoupler. This is done during the pumping phase while the cavity length is ramped. The occurrence of interference peaks are detected by an electronic board which triggers the pockels cell driver [13]. The oscillator laser pulses are transversally modematched to the subsequent first INNOSLAB amplifier stage.

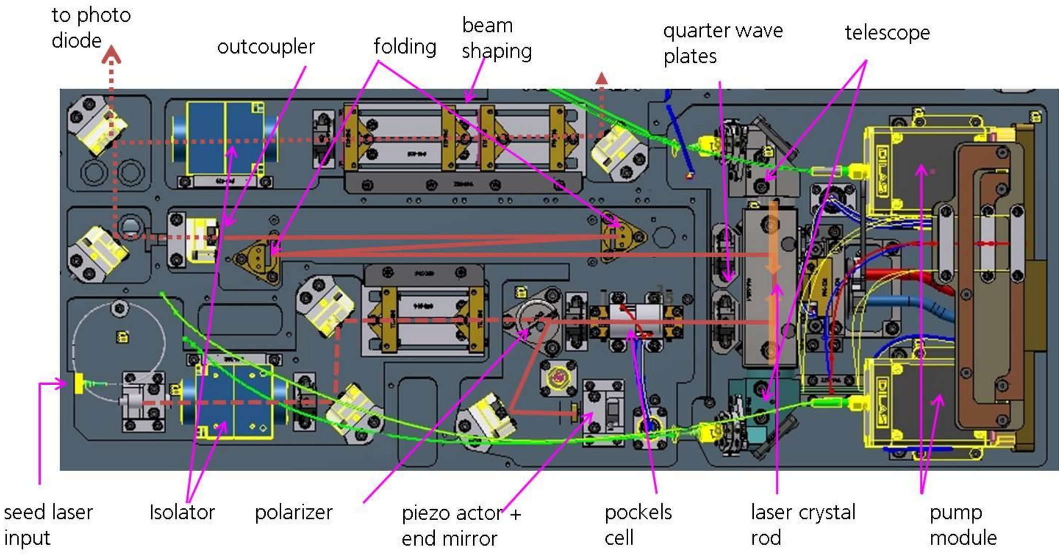

Figure 2-2: setup of the oscillator section

Parameter	**value**
distance crystal <-> outcoupler	690 mm
distance crystal <-> endmirror	222 mm
outcoupler curvature	plane
outcoupler reflectivity	60%
endmirror curvature	concave
endmirror reflectivity	>99%
Laser crystal	Nd:YAG
Nd-doping	0.8 at%
Crystal dimensions	5*5*15 mm^3 (w*h*l)
Type pockelscell	RTP

Table 2-1: oscillator properties of CH_4 and CO_2-system

The setup of the amplifier section is given in Figure 2-3. The pump configuration for the three INNOSLAB stages is identical. A slab shaped Nd:YAG crystal is longitudinally pumped from both ends with identically line shaped pump profiles. While in slow axis (with respect to the diode bars, parallel to the plane of the laser plate) the long side of the optical aperture is fully covered in the perpendicular fast axis the crystal is only partially pumped. The pump light is emitted by passively cooled vertical diode stacks where each of them contains eight fast axis collimated diode bars. The spatial intensity distribution is homogenized in slow axis in order to compensate for inhomogeneous distributions for example in case of emitter failure. The homogenized distribution is subsequently imaged into the crystal. Both large crystal surfaces which are in line with the slow axis are soldered to a copper heat sink form for effective cooling. With this configuration a unidimensional thermal lens is generated perpendicular to the large cooling surfaces. More details about the INNOSLAB-configuration as power amplifier can be found elsewhere [1][2][3].

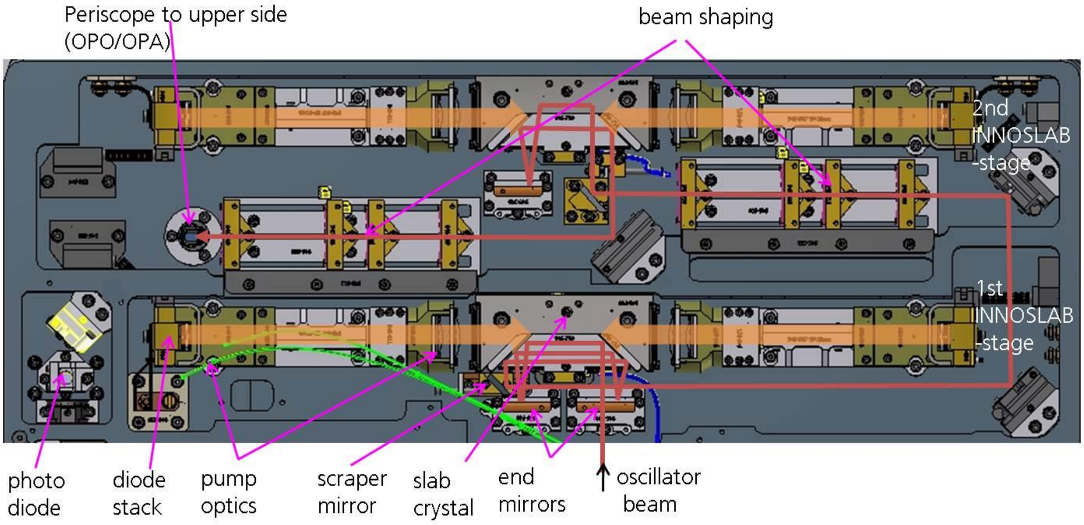

Figure 2-3: setup of the amplifier section

Parameter	Value
Length of cavity	102 mm
Magnification	1^{st} stage: 1.4
	2^{nd} stage: 1
Number of crystal passes	1^{st} stage: 7
	2^{nd} stage: 2
Laser crystal	Nd:YAG
Nd-doping	0.7 at%
Crystal dimensions	18*4*20 mm^3 (w*h*l)
Height of pump line	~1.8 mm

Table 2-2: amplifier properties of both the CH_4 and CO_2-system

In the first amplifier stage the beam coming from the oscillator is propagated through the slab crystal seven times. While the beam size in fast axis (with respect to the diode bars) is constantly matched to the pump height the beam is broadened in slow axis equally for each pass. Therefore, the intensity distribution of the outgoing beam has typically an elliptic shape where the small axis is parallel to the fast axis of the pump diode bars. As the broadening factor is matched to the single pass amplification the fluence and consequently the amplification properties are nearly kept constant for all crystal passes. The design of the beam passes through the first amplifier stage is equal for both the CH_4 and the CO_2 system. In the CH_4 system the beam is geometrically shaped for the subsequent OPO stage. In this case the asymmetric intensity distribution behind the INNOSLAB amplifier has to be transformed into a round distribution by means of cylindrical telescopes. In the CO_2 system the beam is imaged into the second amplifier stage where the whole pump volume is covered by two crystal passes. Again, cylindrical lenses are used in order to obtain a symmetrical intensity distribution suitable for the following frequency converter.

2.2 Mechanical architecture

Although the CO_2-system comes with one more amplifier stage and optional OPA-stages the mechanical structure of the baseplate is equal for both systems (see Figure 2-4). On the bottom side (with respect to the final mounting orientation) the pump laser stages and on the top side the frequency converters (not shown in Figure 2-4) are accommodated. The baseplates were manufactured from solid Al-blocks. The core of the baseplate has a hollow structure which allows for short connection lines for cooling water and all electrical signals. Also the complete pockels cell driver including HV generation and fast switching is accommodated there. All lines are fed to a central connection box where all plug-in connections are located. On the optical sides certain ribs and borders allow for high stiffness. The whole plate is mounted isostatically at three points in order to minimize mechanical deformation. The total mass of the laser head is approximately 52 kg for the CH_4-system and 54 kg for the CO_2-system, respectively.

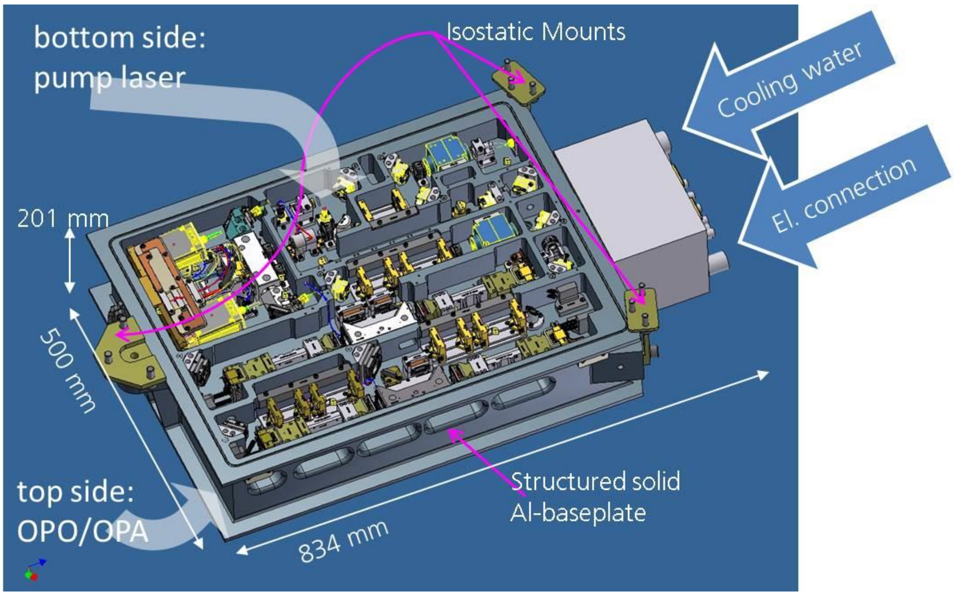

Figure 2-4: mechanical configuration (upside down)

2.3 Rack and Harness

Both lasers are supplied from a single rack that fulfills the requirements for HALO flight equipment (see Figure 2-5). While the diode lasers for pumping of each oscillator and single amplifier stage are all driven by separate modules a single water-air cooler and a central controller unit are shared. A continuous wave fiber based single frequency laser that is used for seeding is mounted inside the controller box. The optical signal is splitted into two equal signals which are propagated to both lasers via polarization maintaining single mode fibers.

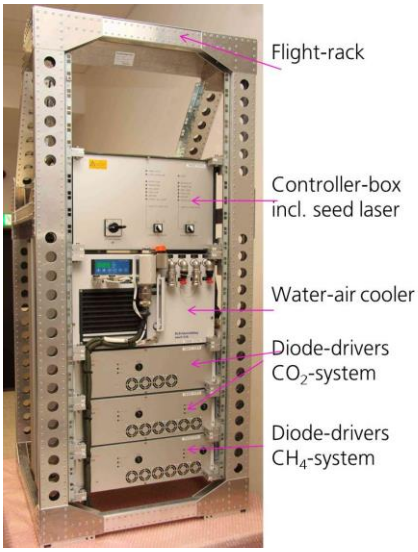

Figure 2-5: Airworthy standard rack containing all supply units for the both lasers

3. PERFORMANCE

The system can be switched between a 100 Hz single pulse and 50 Hz double pulse operation. The latter operation mode reduces the time delay between on-line and off-line pulses and therefore the albedo variation in flight operation. As the temporal separation of two pulses within one pulse pair of currently 500 µs is in the order of magnitude of the storage time of Nd:YAG (~ 230 µs) energy is transferred from the first pumping process to the second pulse. Therefore, there are some slight differences in performance between the different modes. In Table 3-1 the main performance parameters are listed for the double pulse mode. Pulses with about 8 mJ pulse energy and 30 ns pulse duration are generated at nearly diffraction limited beam quality in the oscillators. In both lasers the pulse energy is boosted to about 85 mJ. In the CO_2-system the pulses are amplified in the second amplifier stage to 150 mJ pulse energy. While in the CH_4-system typical values for optical-optical efficiencies of more than 20 % [2] are achieved the actual efficiencies in both amplifier stages of the CO_2-system are substantially lower. An insufficient spectral overlap of the spectral pump light distribution with the absorption lines in Nd:YAG is a potential reason. The beam quality is slightly reduced in all amplifier stages (see Figure 3-1). As no spatial filtering is applied to the beam, INNOSLAB specific Gaussian like intensity distributions with slight side lobes in slow axis are obtained in the far field.

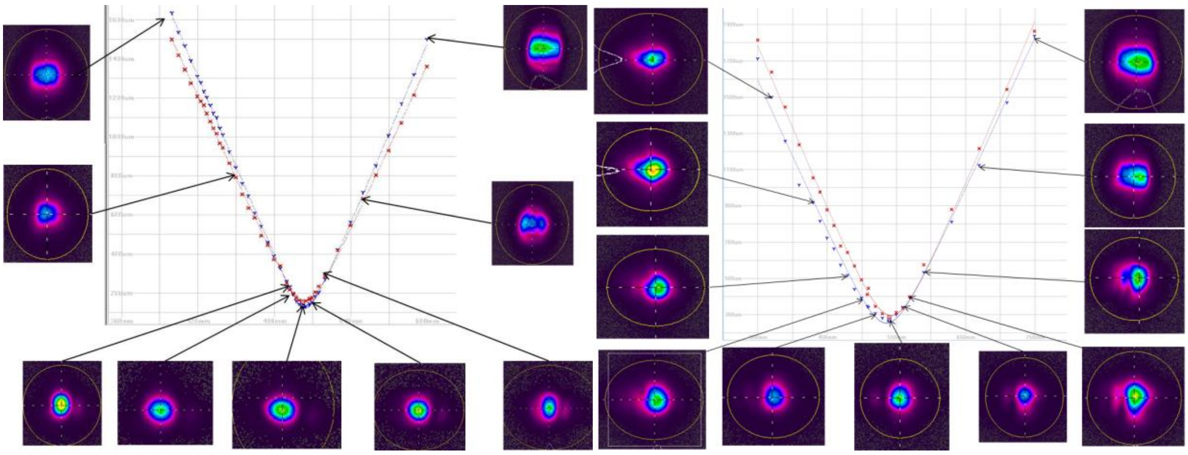

Figure 3-1: Caustic measurements of the outgoing beams behind the last amplifier stage and subsequent geometrical beam shaping. The beam radii measurements were conducted with the 4 sigma method. The intensity profiles are illustrated with pseudo-colors. Left: CH_4-system, Right: CO_2-system.

Parameter	**CH_4-system**	**CO_2-system**
Repetition rate	50 Hz pulse pairs	
Temporal separation of pulses in	500 µs	
Cavity control method	Ramp & fire	
Pulse energy oscillator	8 mJ	8.8 mJ
Pump energy oscillator (behind pump optics)	31.7 mJ	31.5 mJ
oo-efficiency oscillator (*)	25 %	28 %
Pulse energy behind INNOSLAB 1	85 mJ	85 mJ

Pump energy INNOSLAB 1 (behind pump optics)	323 mJ	528 mJ
oo-efficiency INNOSLAB 1 (*)	23.7 %	14.4 % (****)
Pulse energy behind INNOSLAB 2	No 2nd stage	150 mJ
Pump energy INNOSLAB 2 (behind pump optics)	No 2nd stage	528 mJ
oo-efficiency INNOSLAB 2 (*)	No 2nd stage	12.3 % (****)
Pulse duration	~30 ns (fwhm)	~ 30 ns (fwhm)
M^2 oscillator	1.0(**); 1.2(***)	1.0(**); 1.2(***)
M^2 INNOSLAB 1 (small/large axis)	1.3/1.3(**) 1.4/1.6(***)	No measurements due to strong astigmatic beam
M^2 INNOSLAB 2 (small/large axis)	No 2nd stage	1.4/1.7(**) 1.6/2.0(***)

Table 3-1: Overview of beam properties of both systems. (*): oo-efficiency = energy out/ pump energy; energy out: output energy of the oscillator or extracted energy of each amplifier stage, respectively; pump energy: energy behind all pump optics excl. dichroic mirrors; (**): measured with 90/10 knife edge method; (***): measured with 4-sigma method. (****): The optical efficiencies of both INNOSLAB-stages of the CO2-system are substantially lower than typical values. One potential reason is a low spectral overlap between the pump radiation and Nd:YAG absorption lines.

4. SUMMARY AND OUTLOOK

The architecture and performance data of both pump lasers of the CHARM-F system were presented. Both lasers will be used as pump sources for nonlinear frequency converters. The radiation of the CH_4-system has successfully been converted into the measurement wavelength of 1645 nm in a double crystal OPO. About 20 mJ of pulse energy have been generated. Recently, the CO_2-pumplaser was completed. The integration of the OPO/OPA-stages for the conversion into the measurement wavelength at 1572 nm is ongoing. The next steps after the integration of the frequency converters are the integration of both laser sources into the complete CHARM-F-measurement system and the appropriate validation of all relevant beam properties. Here, especially accurate spectral characterization has to be done. In future time the behavior of the laser sources in rough environment has to be tested.

The CH_4-laser that was developed within the CHARM-F-project is an important technology demonstrator for the above mentioned French-German climate mission MERLIN. At present, a preliminary design is being developed for the MERLIN-instrument. Here, it is planned to generate 9 mJ pulse energy at the measurement wavelengths at about 1645 nm. Pump pulses of about 30 to 40 mJ pulse energy will be generated in a similar arrangement where both oscillator and amplifier will be operated at half pulse energy with respect to the CHARM-F-system. More details about the appropriate OPO-converter will be presented in an accompanying presentation and publication [17]. While the optomechanics that were used in the CHARM-F-project are mainly based on clamping, screwing and glueing the MERLIN-optomechanics will be based on screwing and glue-free soldering [14][15][16]. Hereby, the strong requirements concerning environmental conditions and lifetime are intended to be fulfilled. In particular, these are temperature cycles and shocks and low outgassing rates of organic substances.

5. ACKNOWLEDGMENT

This project was funded by DLR space agency as representative for BMBF under contract number FKZ 01LK0905B. The above results were acquired using facilities and devices funded by the Federal State of North-Rhine Westphalia and the European Union within the EFRE-program "Regionale Wettbewerbsfähigkeit und Beschäftigung 2007-2013" under grant number 290047022.

REFERENCES

[1] Russbueldt, P., Mans, T., Weitenberg, J., Hoffmann, H. and Poprawe, R., "Compact diode-pumped 1.1 kW Yb:YAG Innoslab femtosecond amplifier", Opt. Lett. 35, 4169-4171 (2010).

[2] Luttmann J., Nicklaus K., Morasch V., Fu S., Höfer M., Traub M., Hoffmann H.-D., Treichel R., Wührer C. and Zeller P., „Very high-efficiency, frequency-tripled Nd:YAG MOPA for spaceborne lidar“, Proc. SPIE, Vol 6871, 787109 (2008)

[3] Löhring J., Meissner, A., Hoffmann, D., Fix, A., Ehret, G. and Alpers, M., “Diode-pumped single-frequency-Nd:YGG-MOPA for water–vapor DIAL measurements: design, setup and performance”, Applied Physics B: Lasers and Optics, Vol 102, pages 917-935 (2011)

[4] Amediek, A., Büdenbender C., Ehret, G., Fix, A., Kiemle C., Quatrevalet, M., Wirth, M., Hoffmann, D., Kasemann, R., Klein, J., Löhring, J. and Klein, V., "CHARM-F – The Airborne CH_4 and CO_2 IPDA Lidar: Status and Outlook", International Laser Radar Conference, ILRC (2012)

[5] Ehret, G., Fix, A., Amediek, A., Quatrevalet, M., Wirth, M., Löhring, J., Meissner, A., Luttmann, J. and Hoffmann, D., “CHARM-F, the airborne Multi-Wavelength Differential-Absorption Lidar System for the Column-Integrated Dry-Air Mixing Ration XCO_2 and XCH_4”, AGU Fall Meeting, San Francisco, USA (2009)

[6] Quatrevalet, M., Amediek, A., Fix, A., Kiemle, C., Wirth, M., Büdenbender, C., Schweyer, S., Ehret, G., Hoffmann, D., Meissner, A., Löhring, J. and Luttmann, J., “CHARM-F: The Airborne Integral Path Differential Absorption Lidar for Simultaneous Measurements of Atmospheric CO2 and CH4”, 25th International Laser Radar Conference, ILRC, St. Petersburg, Russia (2010)

[7] Amediek, A., Büdenbender, C., Ehret, G., Fix, A., Kiemle, C., Quatrevalet, M., Wirth, M., Hoffmann, D., Kasemann, R., Klein, J., Löhring, J. and Klein, V., “CHARM-F – The Airborne CH_4 and CO_2 IPDA Lidar: Status and Outlook”, Reviewed and Revised Papers presented at the 26th International Laser Radar Conference, ILRC 2012, Vol 1, pages 239-242. International Co-ordination group for Laser Atmospheric Studies. International Laser Radar Conference (ILRC), Porto Heli, Greece (2012)

[8] Wirth, M., Amediek, A., Büdenbender, C., Ehret, G., Fix, A., Kiemle, C., Quatrevalet, M., Hoffmann, D., Löhring, J., Klein, V. and Schöffl, R., “CHARM-F: An airborne Integrated Path Differential Absorption (IPDA) LIDAR for the simultaneous measurement of CO_2 and CH_4 Columns”, AGU Fall Meeting, San Francisco, USA (2011)

[9] Amediek, A., Büdenbender, C., Ehret, G., Fix, A., Kiemle, C., Quatrevalet, M., Wirth, M. Hoffmann, D., Löhring, J. and Klein, V., “Characteristics of an airborne demonstrator for MERLIN”, AGU Fall Meeting, San Francisco, USA (2012)

[10] Fix, A., Büdenbender, C., Wirth, M., Quatrevalet, M., Amediek, A., Kiemle, C. and Ehret, G. “Optical parametric oscillators and amplifiers for airborne and spaceborne active remote sensing of CO_2 and CH_4”, Proc. SPIE 8182, 818206 (2011)

[11] Ehret, G., Flamant, P., Amediek, A., Ciais, P., Gibert, F., Fix, A., Kiemle, C., Quatrevalet, M. and Wirth, M., “The French-German Climate Monitoring Initiative on Global Observations of Atmospheric Methane”, 25th International Laser Radar Conference, ILRC, St. Petersburg, Russia (2010)

[12] Alpers, M., “MERLIN - Die deutsch-französische Klimamission”, DLR, 14 Januar 2014, <http://www.dlr.de/rd/en/desktopdefault.aspx/tabid-2440/3586_read-31672/>

[13] Nicklaus K., Morasch V., Hoefer M., Luttmann J., Vierkötter M., Ostermeyer M. and Höffner J., „Frequency stabilisation of Q-switched Nd:YAG oscillators for airborne and spaceborne LIDAR systems“, Proc. SPIE, Vol 6451, 64511L (2007)

[14] Leers, M., Winzen, M., Liermann, E., Faidel, H., Westphalen, T., Miesner, J., Luttmann, J. and Hoffmann, D., “Highly precise and robust packaging of optical components”, Proc. SPIE, Vol 8244, 824404-824404 (2012)

[15] Faidel H., Gronloh B., Winzen M., Liermann E., Esser D., Morasch V., Luttmann J. Leers M. and Hoffmann D., “Passive alignment and soldering technique for optical components”, Proc. SPIE, Vol. 8235, 82351I (2012)

[16] Leers, M., Winzen, M., Liermann, E., Faidel, H., Westphalen, T., Miesner, J., Luttmann, J. and Hoffmann, D., "Pick and align — High precision active alignment of optical components", Electronic Components and Technology Conference (ECTC), IEEE 62nd , pp.208 (2012)

[17] Livrozet M. J., Elsen F., Wüppen J., Löhring J., Büdenbender C., Fix A., Jungbluth B. and Hoffmann H., "Feasibility and performance study for a space-borne 1645 nm OPO for French-German satellite mission MERLIN", to be published, Proc. SPIE, Paper 8959-17 (2014)